Solution and Surface Effects on Plasma Fibronectin Structure

NANCY M. TOONEY,*‡ MICHAEL W. MOSESSON,* DAVID L. AMRANI,* JAMES F. HAINFELD,§ and JOSEPH S. WALL§

*Department of Medicine (Milwaukee Clinical Campus), University of Wisconsin Medical School, Hemostasis Research Laboratory, Mount Sinai Medical Center, Milwaukee, Wisconsin 53233; ‡Department of Chemistry, Polytechnic Institute of New York, Brooklyn, New York 11201; and §Biology Department, Brookhaven National Laboratory, Upton, New York 11973

ABSTRACT As assessed by electron microscopy, the reported shape of the plasma fibronectin molecule ranges from that of a compact particle to an elongated, rod-like structure. In this study, we evaluated the effects of solution and surface conditions on fibronectin shape. Freeze-dried, unstained human plasma fibronectin molecules deposited at pH 7.0–7.4 onto carbon films and examined by scanning transmission electron microscopy appeared relatively compact and pleiomorphic, with approximate average dimensions of 24 nm × 16 nm. Negatively stained molecules also had a similar shape but revealed greater detail in that we observed irregular, yarn-like structures. Glutaraldehyde-induced intramolecular cross-linking did not alter the appearance of plasma fibronectin. Molecules deposited at pH 2.8, pH 9.3, or after succinylation were less compact than those deposited at neutral pH. In contrast, fibronectin molecules sprayed onto mica surfaces at pH 7, rotary shadowed, and examined by transmission electron microscopy were elongated and nodular with a contour length of 120–130 nm.

Sedimentation velocity experiments and electron microscopic observations indicate that fibronectin unfolds when it is succinylated, when the ionic strength is raised at pH 7, or when the pH is adjusted to 9.3 or 2.8. Greater unfolding is observed at pH 2.8 at low ionic strength (<0.01) compared with material at that pH in 0.15 M NaCl solution. We conclude that (*a*) the shape assumed by the fibronectin molecule can be strongly affected by solution conditions and by deposition onto certain surfaces; and that (*b*) the images of fibronectin seen by scanning transmission electron microscopy at neutral pH on carbon film are representative of molecules in physiologic solution.

'Fibronectin' is the term generally used to describe a family of structurally and immunologically related high molecular weight glycoproteins that are found on many cell surfaces, in extracellular fluids, in connective tissues, and in most basement membranes. One of the universal features of all fibronectin molecules is the presence of distinct binding regions, each typically having a selective affinity for one or another of several different macromolecules such as collagen, fibrin(ogen), other fibronectin molecules, heparin, actin, DNA, and others (1–4). Binding regions also exist for certain mammalian cells (e.g., fibroblasts, monocytes) and for certain bacteria (e.g., *Staphylococcus aureus*) (1–4). These multiple binding sites on fibronectin evidently mediate several biologic "adhesive" activities such as cell to cell adhesion, cell to substrate attachment and spreading, collagen attachment to mononuclear phagocytes and/or to filamentous matrices during formation, and remodeling of connective tissue.

The major circulating form of human plasma fibronectin is a dimer of molecular weight 450,000 (5). The two chains are linked together by disulfide bridges near each carboxy terminus (1–4, 6). The far ultraviolet circular dichroism spectrum gives little evidence of highly ordered secondary structure (5, 7, 8). Plasma fibronectin at neutral pH displays a sedimentation constant ($s_{20,w}$) in the range of 12–14S (5, 7, 9). In contrast, another well characterized plasma protein, fibrinogen (340,000 mol wt), has an axial ratio of 5–1 and a $s_{20,w}$ of only 7–8S (10). This large difference in their sedimentation coefficients indicates that fibronectin has a relatively

THE JOURNAL OF CELL BIOLOGY · VOLUME 97 DECEMBER 1983 1686–1692
© The Rockefeller University Press · 0021-9525/83/12/1686/07 $1.00

Downloaded from http://rupress.org/jcb/article-pdf/97/6/1686/1641953/1686.pdf by guest on 17 April 2024

lower frictional resistance, hence a smaller axial ratio. The $s_{20,w}$ of plasma fibronectin falls markedly in the presence of urea (5), as the pH is raised (7, 9), in the presence of heparin at 4°C (11), or in high salt (12). This behavior suggests an increase in frictional resistance to sedimentation brought about by unfolding and extension from a more compact shape.

Evidence to corroborate the conformational state(s) of plasma fibronectin molecules has been sought by electron microscopy. Images obtained by Koteliansky et al. (13) of freeze-dried, rotary-shadowed plasma fibronectin specimens deposited at physiologic pH suggested moderately compact ellipsoidal shapes (~16 × 9 nm). Vuento et al. (14) reported seeing irregularly shaped particles resembling pieces of "coiled thread extending to a certain degree". In the presence of polyamines, they could induce these molecules to form filamentous polymers. These latter forms resemble the familiar fibrillar network that is characteristic of extracellular fibronectin matrices (15–17).

In contrast to the results reported by Koteliansky et al., the images reported by Engel et al. (18), Odermatt et al. (8), and Erickson et al. (19) indicate a considerably more extended shape for the native molecule. These investigators observed curvilinear flexible particles ~120 nm in contour length and ~2 nm in diameter; a small proportion of the images seen by Erickson et al. (19) were reportedly more folded. Recently, these investigators have suggested that ionic strength affects the degree of unfolding (20). Price et al. (21) reported that tungsten-shadowed fibronectin molecules that had been sprayed onto carbon films appeared as randomly coiled strands with dimensions of ~51 × 32 nm. In contrast, molecules deposited on polystyrene surfaces appeared to be nodular, rod-like structures 130 nm long.

We have attempted to determine factors affecting the shape of the fibronectin molecule in solution by comparing electron microscope images of freeze-dried plasma fibronectin molecules that had been deposited from drops on carbon films under various aqueous solvent conditions with images of samples sprayed from glycerol solutions onto mica. Ultracentrifugal behavior was also examined under selected solvent conditions. Our results form the basis for this report.

MATERIALS AND METHODS

Preparation of Plasma Fibronectin: Human plasma fibronectin was purified from the heparin-precipitable fraction of plasma (22). The protein was stored at −70°C as a stock solution of 1–4 mg/ml in 0.1 M Tris-phosphate buffer, pH 7.4. For certain experiments, "Zone I" fibronectin dimers were separated from lower molecular weight fibronectin by Sepharose 6B-CL chromatography as described by Amrani et al. (22). Fibronectin prepared by elution from gelatin-Sepharose with 8 M urea (23) was the gift of Dr. J. M. McDonald, Washington University, St. Louis. Samples of fibronectin, prepared by adsorption of plasma cryoprecipitate on gelatin-Sepharose followed by elution with potassium bromide, were the gift of Dr. B. Horowitz, New York Blood Center (unpublished method).

Cross-linking of purified plasma fibronectin with glutaraldehyde was carried out as previously described for fibrinogen (24). The protein concentration was 0.25–0.5 mg/ml, while the glutaraldehyde concentration was varied from 0.1–0.25%.

Succinylation (25) of fibronectin was carried out at pH 9 using a 10-fold molar excess of succinic anhydride to lysine. These samples were dialyzed against 0.15 M NaCl, 0.02 M *N*-tris(hydroxymethyl)methyl-2-aminoethane sulfonic acid (TES)[1], pH 7.2, and stored.

[1] *Abbreviations used in this paper:* STEM, scanning transmission electron microscopy; TES, *N*-tris(hydroxymethyl)methyl-2-aminoethane sulfonic acid.

Electrophoretic Analysis: SDS PAGE (26) of unreduced plasma fibronectin in 4 or 5% polyacrylamide gels displayed a main band, comprising ~95% of the total material in a position corresponding to the fibronectin dimer (molecular weight ~450,000; reference 5). The remainder migrated mainly in a position corresponding to smaller fibronectin polypeptide chains and molecular fragments (molecular weight range of 190,000–235,000; references 27, 28). Most material migrated in a position corresponding to a monomer molecular weight in the range of 220,000, as is characteristic of fibronectin after reduction of disulfide bridges (5).

Scanning Transmission Electron Microscopy: High resolution scanning transmission electron microscopy (STEM) was performed at the Brookhaven STEM Biotechnology Resource using a 40 kV probe as previously described (24). The preparation of thin carbon films and the method of specimen application for freeze-drying or negative contrasting have been reported (24). Final protein concentrations varied from 5 to 10 μg/ml. Fibronectin samples were diluted into ammonium acetate (pH 7.0), ammonium carbonate (pH 9.3), 1% acetic acid (pH 2.8), 0.13 M NaCl, 0.02 M Tris buffer, pH 7.4, or 0.15 M NaCl, 0.02 M TES buffer, pH 7.2, for deposition on carbon films. First, tobacco mosaic virus was deposited on grids in 10 nM ammonium acetate at a nominal concentration of 30 μg/ml. The grid was then washed with buffer and the sample solution was injected into the buffer droplet. A 2% solution of uranyl sulfate was used as a negative contrasting agent, as required.

Transmission Electron Microscopy: A Philips 400 transmission electron microscope operating at 60 or 80 kV was used with a 30 micron objective aperture. Fibronectin samples were diluted into a solution prepared by mixing 1 vol of glycerol with 1 vol of 0.2 M ammonium acetate, pH 7.0, to concentrations of 30–50 μg/ml and sprayed onto freshly cleaved mica surfaces. Rotary shadowing was carried out in a Balzers high vacuum coating apparatus (Balzers, Hudson, NH) using an electron beam gun with a platinum-carbon electrode. The nominal shadowing angle was ~10°. Specimens were then coated with carbon at 90° and the films were floated off onto water and picked up on copper grids.

Mass Analyses: The mass analysis of freeze-dried, unstained molecules was carried out according to Hainfeld et al. (29). Molecular weight values are expressed as the mean ± 1 SD.

Analytical Ultracentrifugation: Sedimentation velocity measurements were carried out as previously described (5) using a Beckman Model E analytical ultracentrifuge (Beckman Instruments, Inc. Palo Alto, CA) equipped with schlieren optics. Fibronectin (1–7 mg/ml) was dialyzed into 0.15 M NaCl, 0.02 M TES, pH 7.2, unless otherwise noted.

Isoelectric Point: Solubility studies of plasma fibronectin were carried out to determine its isoelectric point by dialyzing a solution of this protein (6.8 mg/ml) in 0.1 M Tris-phosphate buffer, pH 7.0, at 5°C against low ionic strength (I = 0.005–0.01) acetate or phosphate buffers (5 mM acetic acid adjusted to pH 4–5.4 with sodium hydroxide or 5 mM phosphoric acid adjusted to pH 6.0–7.0 with sodium hydroxide). The amount of material remaining in the supernatant solution after centrifugation at 5°C was determined spectrophotometrically at 280 nm assuming an absorbance of 12.8 for a 1% solution in a 1-cm path-length cell (30).

RESULTS

Plasma Fibronectin at Physiological pH

As determined by STEM analysis, plasma fibronectin, deposited at pH 7.0–7.4 in the presence or absence of glycerol on glow-discharged thin carbon films and subsequently freeze dried, revealed relatively compact, pleiomorphic shapes. The particles appeared irregular in shape and were ~16 nm in their shortest dimension and up to 24 nm in the longest dimension (Fig. 1, *a–c*). Fig. 1 *c* shows the pleiomorphic nature of the images. We obtained the same results with several different fibronectin specimens that had been prepared by different methods (see Materials and Methods). Most human plasma fibronectin (95%) consists of dimeric molecules, 450,000 mol wt, whereas about 5% circulates as smaller molecular weight polypeptides, 190,000–235,000 (27). To obtain a population consisting only of dimeric 450,000-mol-wt molecules (i.e., Zone I fibronectin) some samples were subfractionated by Sepharose 6B-CL chromatography (22).

Plasma fibronectin is precipitated in the cold in the presence of heparin or fibrinogen/fibrin complexes (31, 32), suggesting

Downloaded from http://rupress.org/jcb/article-pdf/97/6/1686/1641953/1686.pdf by guest on 17 April 2024

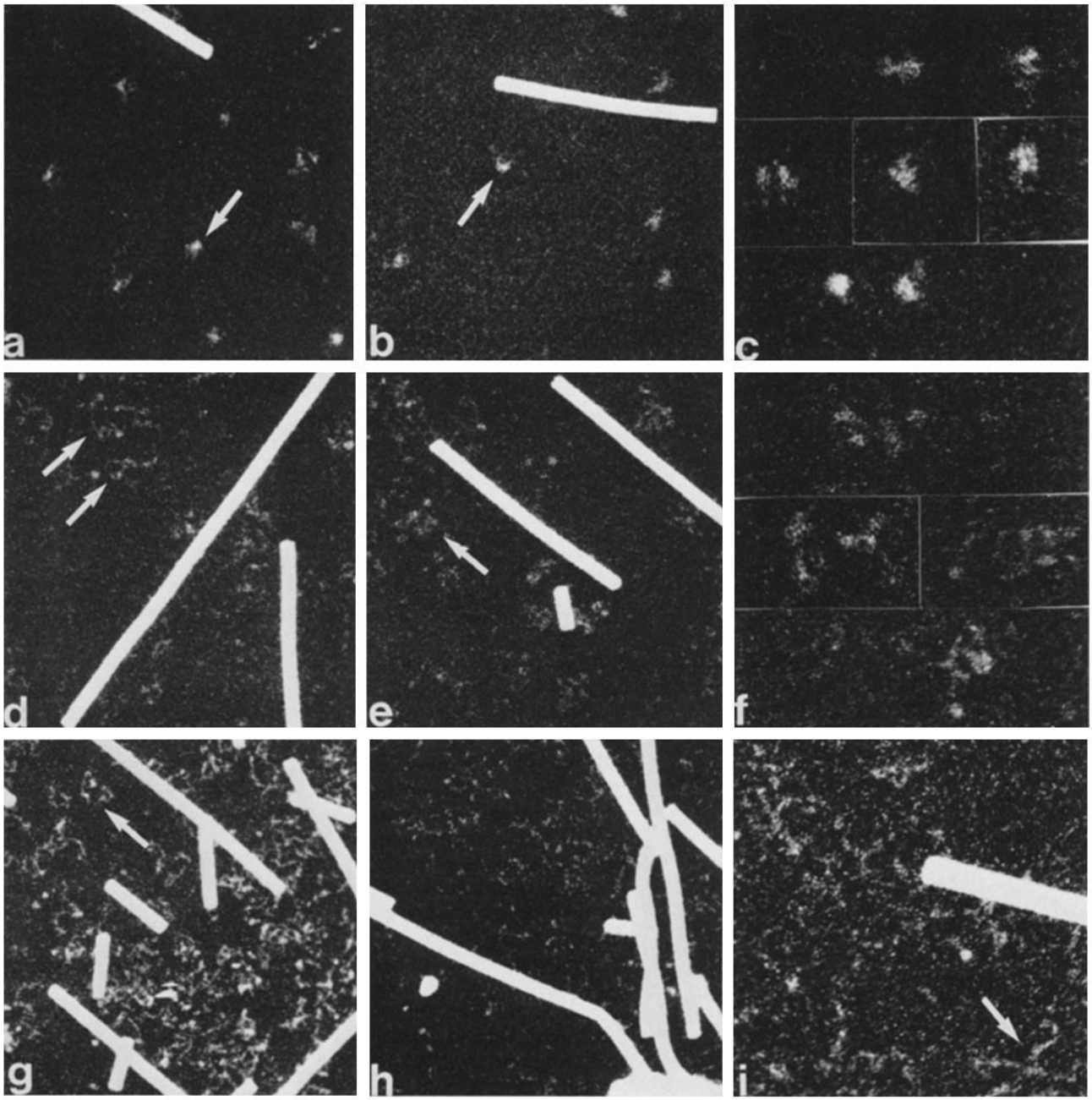

FIGURE 1 STEM Images of freeze-dried fibronectin. All samples were deposited on grids at ambient temperature, except where noted. The rod-like forms are TMV, included for purposes of mass calibration (24, 27). Image intensities are directly related to mass distribution. (*a*) Fibronectin was deposited in 0.13 M NaCl, 0.02 M Tris buffer, pH 7.4, onto thin carbon films at ambient temperature under conditions described in reference 21. The arrow points to a typical particle of molecular weight ~440,000, as evaluated by a "circle" program (24, 27). The average dimensions for such images were 16 × 24 nm, but there was considerable variability in shape. Dimensions as short as 12 nm and as long as 32 nm were occasionally seen for these images. × 125,000. (*b*) Fibronectin deposited at 2°C under conditions described in *a*. No effect of low temperature was observed under these conditions. The arrow indicates a typical particle. × 125,000. (*c*) Selected images of fibronectin deposited at ambient temperature using conditions described in *a*. Note the relatively compact, pleiomorphic shape. × 251,000. (*d* and *e*) Fibronectin deposited in 0.2 M ammonium carbonate buffer, pH 9.3, under conditions described for *a* and *b*. The arrows show typical 440,000-mol-wt particles, determined with the "user-defined boundaries" program. The particles are more expanded and extended than those in *a*–*c*. × 125,000. (*f*) Selected images of fibronectin deposited under conditions described in *d* and *e*. Note that the images are more expanded and extended than those in *c*. × 251,000. (*g*) Succinylated fibronectin deposition in 0.2 M ammonium acetate, pH 7.0. Unmodified fibronectin (not shown) applied under these conditions gave images indistinguishable from those shown in *a*–*c*. The arrow points to an image of an individual molecule, as judged by mass analysis. (*h*) Fibronectin deposited in 1% acetic acid, pH 2.8, as described in *a*. Note the similarity to images obtained at pH 9.3. × 125,000. (*i*) Fibronectin deposited as described in *h*. The arrow shows an unfolded single molecule, as judged by mass analysis. × 251,000.

Downloaded from http://rupress.org/jcb/article-pdf/97/6/1686/1641953/1686.pdf by guest on 17 April 2024

that the fibronectin molecule may undergo temperature-dependent shape changes. To determine whether such changes were observable by STEM techniques, samples were deposited on grids at room temperature or at 2°C before freeze drying. No changes were observed in the images obtained (compare Fig. 1, *a* and *b*).

Mass measurements on plasma fibronectin were initially made with a "circle" program, where the background is subtracted from the integrated intensity within a circle and tobacco mosaic virus is used as a mass calibration standard (29). More recently, a program for tracing "user-defined boundaries" has also been used (29) so that the boundaries of molecules could be followed more closely. The mass of Zone I fibronectin molecules, as assessed by the "circle" program, was 460,000 ± 120,000 mol wt (n = 301). Data from the analysis of fibronectin molecules, prepared either by the heparin precipitation method or by either of the gelatin-Sepharose affinity methods showed no significant difference from this value (i.e., 434,000 ± 103,000 mol wt [n = 100]). The relatively large standard deviation (~25%) for these measurements may be related to using a circle for defining the mass of irregularly shaped particles, a procedure that includes excess background area. A smaller sample (n = 11) of fibronectin molecules was measured with the "user-defined boundaries" program. The mean value obtained was 450,000 ± 50,000 mol wt (11%). These values suggest that careful application of user-defined contouring may give more precise results than the circle program, although this procedure is considerably more tedious to carry out.

In contrast to the shapes obtained for fibronectin molecules deposited on glow-discharged carbon films, samples of fibronectin sprayed onto mica surfaces produced molecules that were more extended and elongated (Fig. 2). The length of these molecules, 120–130 nm, is similar to that reported by other investigators under comparable conditions (8, 18, 19, 21).

Several investigators have correlated solution properties of plasma fibronectin with electron microscopic observations, chiefly using sedimentation velocity measurements. Odermatt et al. (8) calculated that if plasma fibronectin were a hydrodynamically compact sphere, its $s^{\circ}_{20,w}$ value would be in excess of 20S. The experimentally observed $s^{\circ}_{20,w}$ is in the range of 13S for solutions at physiological ionic strength and pH, suggesting that the molecule either is not fully compact or is somewhat asymmetric. We observed no major changes in $s^{\circ}_{20,w}$ when it was evaluated as a function of temperature (Fig. 3); the extrapolated $s^{\circ}_{20,w}$ at 37°C is essentially the same as that at 4°C, namely 13.5S. At any given protein concentration, $s_{20,w}$ values were slightly greater at 4°C than at 37°C. The slope of $s_{20,w}$ versus concentration at 37°C was slightly negative (−0.18), as has been reported at ambient temperature (7); whereas, at 4°C, the slope was slightly positive (+0.18), suggesting that the molecules may have a tendency to self-aggregate at this temperature.

Plasma Fibronectin at pH 9.3 or 2.8

STEM (Fig. 1, *d–f, h,* and *i*) and sedimentation velocity measurements (Table I) were used to evaluate the effects of pH and ionic strength on the molecule measured above and below the isoelectric point (pH 5.2 ± 0.2, Table II). STEM images of samples in 0.2 M ammonium carbonate, pH 9.3, were clearly less compact than samples deposited at pH 7.4 (Fig. 1, *d–f*), as is clearly seen by comparing individual

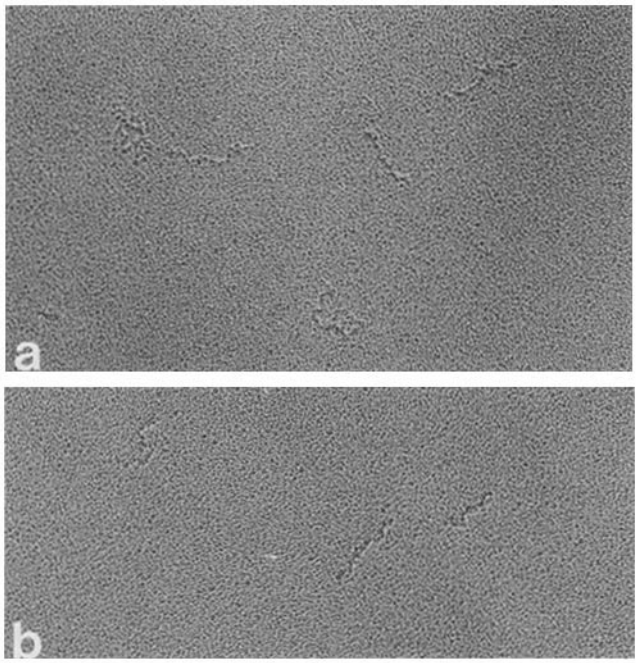

FIGURE 2 Transmission electron microscopy images of fibronectin. Samples were diluted into a solution containing one part glycerol and one part 0.2 M ammonium acetate, pH 7 (vol/vol), sprayed onto freshly cleaved mica, and rotary shadowed with platinum-carbon. The molecules prepared in this manner are more extended than those prepared at pH 7 shown in Fig. 1, *a–c*. × 100,000.

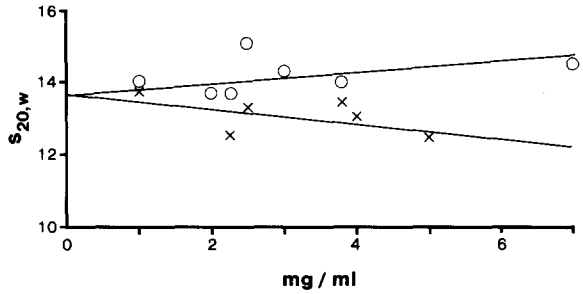

FIGURE 3 The sedimentation coefficient of fibronectin. Samples were dialyzed into 0.15 M NaCl, 0.02 M TES buffer, pH 7.2. The slopes and intercepts of the lines were determined by regression analysis. O, 4°C; X, 37°C.

molecules in Fig. 1, *f* and *c*. This unfolding effect was reversible, as judged from images of samples exposed to buffer at pH 9.3 and then dialyzed back into pH 7.2 buffer. Consistent with the unfolding seen by STEM (Fig. 1, *d–f*) and with previous reports on reduction of $s_{20,w}$ at alkaline pH (7, 9), the $s_{20,w}$ of plasma fibronectin (6 mg/ml) at pH 9.3 fell to 7.6S (Table I). Furthermore, the boundary of the sedimenting peak at pH 9.3 was much sharper than that forming at pH 7.2, indicating that the molecule at pH 9.3 had undergone a change in shape resulting in slower diffusion.

STEM images of samples prepared in dilute acetic acid, pH 2.8, were even more unfolded and extended than the images obtained at pH 9.3 (Fig. 1, *h* and *i*). Such unfolding was also documented by the observed reduction in the $s_{20,w}$ to 4.8 (Table I). In the presence of 0.15 M NaCl, the change at low pH was less dramatic in that the $s_{20,w}$ was 10.3S, and the STEM images (not shown) resembled those observed at pH 9.3. This change in $s_{20,w}$ also was reversible by dialyzing the

Downloaded from http://rupress.org/jcb/article-pdf/97/6/1686/1641953/1686.pdf by guest on 17 April 2024

TABLE I

Sedimentation Coefficient of Fibronectin

Conditions*	Ionic strength	$s_{20,w}$
0.02 M TES, 0.15 M sodium chloride, pH 7.4	0.17	13.5
0.02 M TES, 0.75 M sodium chloride, pH 7.4	0.77	6.7
0.2 M ammonium bicarbonate, pH 9.3	0.22	7.6
1% acetic acid, pH 2.8	<0.01	4.8
0.02 M acetic acid, 0.15 M NaCl, pH 3.0	0.15	10.3
Succinylated, in 0.2 M ammonium bicarbonate, pH 7.0	0.20	7.5

* The sample concentrations were ~2 mg/ml except for the pH 9.3 sample, which was measured at a concentration of 6 mg/ml. Buffers were generally selected to duplicate conditions used for electron microscopy.

TABLE II

Estimation of the Isoelectric Point of Fibronectin by Solubility Measurement

pH	Supernatant protein concentration
	mg/ml
4.0	3.44
4.5	2.63
5.0	0.22
5.4	0.22
5.9	1.56
6.5	2.54
7.0	3.31

Fibronectin (6.8 mg/ml) in 0.1 M Tris phosphate buffer, pH 7.0, was dialyzed at 5°C against 5 mM acetate or phosphate buffers of pH 4–7.0. The concentration of material remaining in solution at each pH is indicated. Based upon the observed solubilities, we estimate the isoelectric point of plasma fibronectin to be pH 5.2 ± 0.2.

pH 2.8 sample back into pH 7.2 buffer. STEM images of such dialyzed material were indistinguishable from those obtained by direct application of samples at pH 7.2.

Plasma Fibronectin at High Ionic Strength

The sedimentation coefficient of plasma fibronectin in TES buffer decreased from 13.5 to 6.7 when the sodium chloride concentration was increased from 0.15 M to 0.75 M (Table I). These findings are consistent with the changes in $s_{20,w}$ and $D_{20,w}$ reported by Williams et al. (12).

Chemically Modified Plasma Fibronectin

GLUTARALDEHYDE FIXATION: As assessed by SDS PAGE, untreated dimeric fibronectin samples are converted to monomeric subjects after disulfide bridge reduction (Fig. 4, *b* and *d*). That is, the molecular weight is reduced from 450,000 to ~220,000. In contrast, samples that had been glutaraldehyde-fixed showed no change in mobility after reduction and only a small proportion of the sample appeared multimeric (Fig. 4, *a* and *c*). Thus, reaction of plasma fibronectin with glutaraldehyde evidently results in internal fixation of the polypeptide chains comprising each dimeric fibronectin molecule without extensive intermolecular covalent bridging.

STEM images of glutaraldehyde-treated, unreduced samples deposited at pH 7.2 did not differ significantly from untreated material. Negatively contrasted images of control or glutaraldehyde-treated samples confirmed the loosely folded shape observed for freeze-dried specimens, but showed somewhat greater structural detail, in that we observed a knobby, yarn-like image (Fig. 5, *a* and *b*).

SUCCINYLATED PLASMA FIBRONECTIN: The $s_{20,w}$ of succinylated fibronectin in 0.15 M NaCl, 0.02 M TES buffer, pH 7.2, was 7.5S (Table I) and the observed peak was hypersharp. Under these conditions, there was little, if any, change in the circular dichroism spectrum as a consequence of succinylation (data not shown), suggesting that the secondary structure of the molecule was largely unchanged by this treatment. However, STEM images of this freeze-dried material deposited at pH 7.2 (Fig. 1 *g*) indicate that the introduction of negative charges destabilizes the folding of the molecule. That is, the molecules of succinylated fibronectin appeared much more extended and rope-like than did unsuccinylated samples at the same pH.

DISCUSSION

Our STEM images of plasma fibronectin obtained from freeze-dried solutions deposited at physiological ionic strength and pH show that the molecule tends to be relatively compact and pleiomorphic in shape. STEM images differ from conventional transmission electron microscopy images in that there is no enhancement of contrast by staining or shadowing. Hence, image intensity is directly related to mass distribution. Negatively contrasted STEM images show greater molecular detail, with a loosely folded, knobby, yarn-like structure. The average dimensions of freeze-dried molecules, roughly 16 × 24 nm, are greater than those reported by Koteliansky et al. (16 × 9 nm, reference 10), but smaller than those reported by Price et al. (51 × 32 nm, reference 21). Koteliansky et al. prepared specimens from 0.05 M ammonium acetate, pH 7.5, at relatively high protein concentration (13). It is difficult

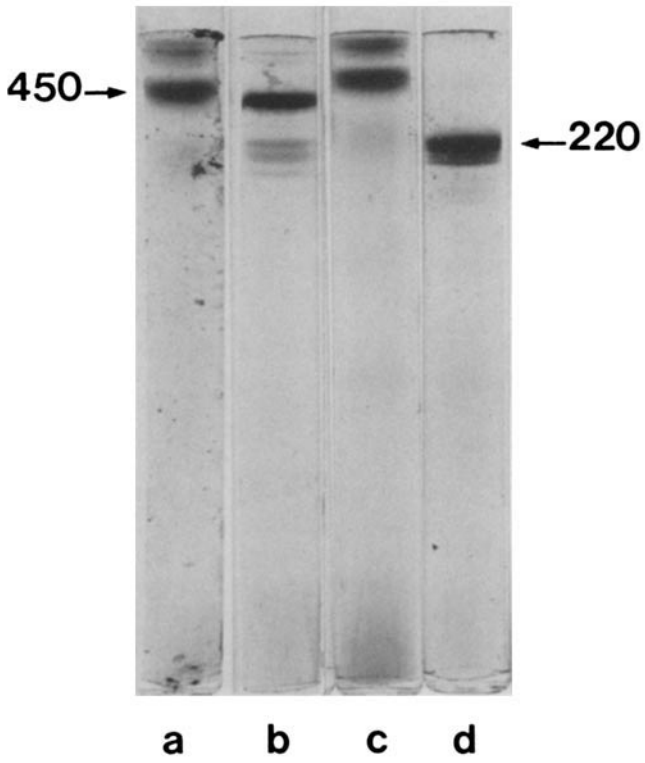

FIGURE 4 SDS PAGE of plasma fibronectin and glutaraldehyde-treated fibronectin. (*a*) Glutaraldehyde-treated fibronectin, unreduced; (*b*) fibronectin, unreduced; (*c*) glutaraldehyde-treated fibronectin, reduced; (*d*) fibronectin, reduced.

Downloaded from http://rupress.org/jcb/article-pdf/97/6/1686/1641953/1686.pdf by guest on 17 April 2024

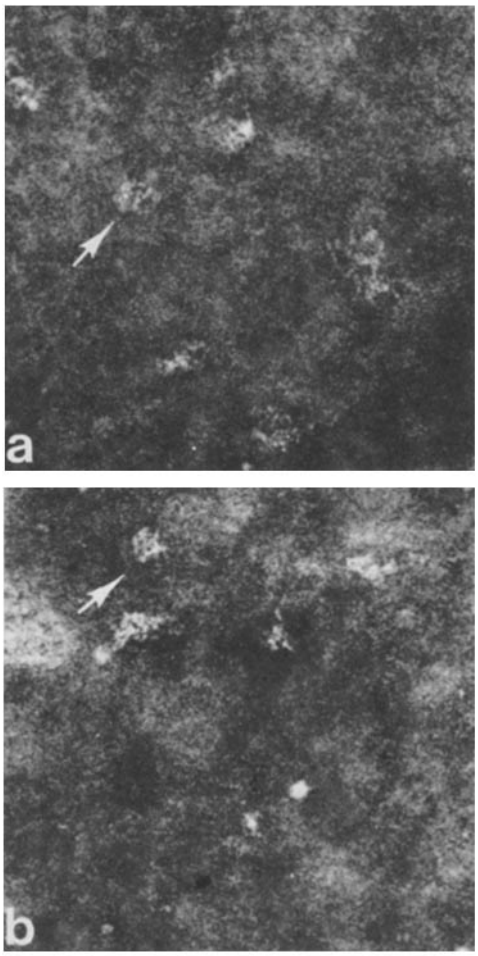

FIGURE 5 STEM images of negatively contrasted plasma fibronectin. (a) Unmodified; (b) glutaraldehyde-treated. Arrows point to typical molecules. Compare these images with those in Fig. 1c. × 251,000.

to discern discrete molecules in Koteliansky's micrographs because of the dense packing of protein. Price et al. (21) used samples diluted into ammonium formate (molarity not specified) or 0.1 M ammonium bicarbonate (pH unspecified), sprayed onto carbon films, air-dried, and shadowed with tungsten. These divergent results emphasize the sensitivity of the fibronectin molecule to surfaces, solution conditions, and air-liquid interfaces.

Images of molecules prepared by freeze-drying on carbon films (Fig. 1, *a–c*) are considerably less extended than images of molecules sprayed from glycerol solution onto mica (18, 19, and Fig. 2). Under these conditions, the molecule evidently unfolds or extends on contact with the polar mica surface. Although glycerol did not markedly affect the appearance of molecules deposited on carbon surfaces (data not shown) we cannot exclude the possibility that it might contribute to the unfolding of the molecule on mica surfaces.

Mass analysis of freeze-dried fibronectin samples proves that the folded forms shown in Fig. 1, *a–c* represent dimeric fibronectin molecules, molecular weight ~450,000. The average mass value is in the molecular weight range determined for samples in solution (8). Our experiments using glutaraldehyde fixation of fibronectin (Figs. 4 and 5) also indicate that plasma fibronectin molecules are folded in solution under physiological conditions.

Flexibility of the fibronectin molecule as a function of pH and ionic strength is shown both by STEM images and by sedimentation velocity measurements. Shifting the pH to 9.2 or to 2.8, two to three pH units on either side of the isoelectric point (pH 5.2 ± 0.2, Table II), promoted a significant shape change, as did increasing sodium chloride concentration to 0.75 M. The shape change in acetic acid at pH 2.8 appears to result from a combination of low ionic strength (<0.01) as well as low pH. Fibronectin molecules at these pHs are less compact than those observed at physiological pH (Fig. 1, *d–h*). Changes in the sedimentation coefficient observed under these buffer conditions (Table I) are consistent with the conclusion that the electron microscopic images indicate molecular expansion and extension, such as had been previously reported for samples unfolded in urea or guanidinium hydrochloride solutions (5, 7). Succinylation produces molecules bearing more negative charges at physiological pH than do unmodified molecules, and also results in molecular unfolding, as assessed by sedimentation velocity experiments and direct STEM observation. It is worth noting that the images shown in Fig. 1, *a–i* were all obtained using approximately the same protein concentration. The comparison of *a–c* and *d–i* leads us to infer that the molecule may be more self-interactive and surface-interactive in its unfolded form.

No major effects of temperature on the shape of the molecule were observed for plasma fibronectin deposited at 2°C on carbon films, compared with ambient temperature. We also did not observe significant effects on the $s^{\circ}_{20,w}$ at 2° or 37°C. We would anticipate that major, temperature-dependent shape changes would occur at elevated temperatures (e.g., 55°C) where previous studies have indicated changes in both the circular dichroism spectrum and fluorescence spectrum (7) and melting determined by differential scanning calorimetry (33). The slightly positive concentration-dependent slope found at 4°C suggests that some self-aggregation may be occurring at this temperature. This observation is consistent with the data of Rocco et al. (34) whose measurements of changes in diffusion properties were similarly interpreted.

We believe the folded structures that we, in this study, and others (20, 21) have observed reflect a shape that is representative of molecules in solution. The two polypeptide chains of plasma fibronectin are linked by disulfide bridges near the carboxy terminal region (1–4, 6). Thus, it is not surprising that the molecule is flexible and can be affected by the nature of the surface on which it is deposited. Folding and unfolding of fibronectin may be important for the expression of certain of its biological activities.

We thank Julie Erickson for skillful secretarial assistance, Doreen Diekfuss for art work, James DiOrio for transmission electron microscopy support, and Martha Bushlow for photographic assistance. We are grateful to Kristin Chung, Frank Kito, and Dr. James Lipka for assistance at the STEM facility.

This work was supported by National Heart, Lung, and Blood Institute program project grant HL 28444, the U. S. Department of Energy, and National Institutes of Health Biotechnology Resource Grant RR 00715.

This paper appeared in abstract form (35) and was presented in part at the twenty-third annual meeting of the American Society for Cell Biology, 2 December 1983.

Received for publication 28 April 1983, and in revised form 1 August 1983.

Downloaded from http://rupress.org/jcb/article-pdf/97/6/1686/1641953/1686.pdf by guest on 17 April 2024

REFERENCES

1. Yamada, K. M., and K. Olden. 1978. Fibronectins—adhesive glycoproteins of cell surface and blood. *Nature (Lond.)*. 275:179–184.
2. Mosesson, M. W., and D. L. Amrani. 1980. The structure and biological activities of plasma fibronectin. *Blood*. 56:145–158.
3. Mosher, D. F. 1980. Fibronectin. *Prog. Hemostasis Thromb.* 5:111–151.
4. Hynes, R. O., and K. M. Yamada. 1982. Fibronectins: multifunctional modular glycoproteins. *J. Cell. Biol.* 95:369–377.
5. Mosesson, M. W., A. B. Chen, and R. M. Huseby. 1975. The cold-insoluble globulin of human plasma: studies of its essential features. *Biochim. Biophys. Acta* 386:509–524.
6. Wagner, D. D., and R. O. Hynes. 1980. Topological arrangement of the major structural features of fibronectin. *J. Biol. Chem.* 255:4304–4312.
7. Alexander, S. S., Jr., G. Colonna, and H. Edelhoch. 1979. The structure and stability of human plasma cold-insoluble globulin. *J. Biol. Chem.* 254:1501–1505.
8. Odermatt, E., J. Engel, H. Richter, and H. Hörmann. 1982. Shape, conformation and stability of fibronectin fragments determined by electron microscopy, circular dichroism and ultracentrifugation. *J. Mol. Biol.* 159:109–123.
9. Miekka, S. I., K. C. Ingham, and D. Ménaché. 1982. Rapid methods for isolation of human plasma fibronectin. *Thromb. Res.* 27:1–14.
10. Shulman, S. 1953. The size and shape of bovine fibrinogen. Studies of sedimentation, diffusion and visocity. *J. Amer. Chem. Soc.* 75:5846–5852.
11. Mortillero, J., D. L. Amrani, M. W. Mosesson, and N. M. Tooney. 1982. Low temperature effects on plasma fibronectin. *Biophys. J.* 37:250*a*. (Abstr.)
12. Williams, E. C., P. A. Janmey, J. D. Ferry, and D. F. Mosher. 1982. Conformational states of fibronectin effects of pH, ionic strength and collagen binding. *J. Biol. Chem.* 257:14973–14978.
13. Koteliansky, V. E., M. A. Glukhova, M. V. Benjanian, V. N. Smirnov, V. V. Filimonov, O. M. Zalite, and S. Y. Venyaminov. 1981. A study on the fine structure of fibronectin. *Eur. J. Biochem.* 119:619–624.
14. Vuento, M., T. Vartio, M. Saraste, C.-H. Von Bonsdorff, and A. Vaheri. 1980. Spontaneous and polyamine-induced formation of filamentous polymers from soluble fibronectin. *Eur. J. Biochem.* 105:33–42.
15. Chen, L. B., A. Murray, R. A. Segal, A. Bushnell, and M. L. Walsh. 1978. Studies of intercellular LETS glycoprotein matrices. *Cell*. 14:377–391.
16. Wartiovaara, J., E. Linder, E. Ruoslahti, and A. Vaheri. 1974. Distribution of fibroblasts surface protein. Association with fibrillar structures of normal cells and loss upon viral transformation. *J. Exp. Med.* 140:1522–1533.
17. Furcht, L. T., D. F. Mosher, and G. Wendelschafer-Crabb. 1978. Immunocytochemical localization of fibronectin (LETS protein) on the surface of L6 myoblasts: light and electron microscopic studies. *Cell*. 13:263–271.
18. Engel, J., E. Odermatt, A. Engel, J. A. Madri, H. Furthmayr, H. Rohde, and R. Timpl. 1981. Shapes, domain organization and flexibility of laminin and fibronectin, two multifunctional proteins of the extracellular matrix. *J. Mol. Biol.* 150:97–120.
19. Erickson, H. P., N. Carrell, and J. McDonagh. 1981. Fibronectin molecule visualized in electron microscopy: a long, thin, flexible strand. *J. Cell Biol.* 91:673–678.
20. Erickson, H. P., and Carrell, N. 1983. Extended and collapsed conformations of fibronectin demonstrated by sedimentation and electron microscopy. *Biophys. J.* 41:237*a*. (Abstr.)
21. Price, T. M., M. L. Rudee, M. Pierschbacher, and E. Ruoslahti. 1982. Structure of fibronectin and its fragments in electron microscopy. *Eur. J. Biochem.* 129:359–363.
22. Amrani, D. L., G. A. Homandberg, N. M. Tooney, C. Wolfenstein-Todel, and M. W. Mosesson. Purification and analysis of the herogeneous forms of plasma fibronectin. *Biochim. Biophys. Acta*. In press.
23. Engvall, E., and E. Ruoslahti. 1977. Binding of soluble form of fibroblast protein, fibronectin, to collagen. *Int. J. Cancer*. 20:1–5.
24. Mosesson, M. W., J. Hainfeld, R. H. Haschemeyer, and J. Wall. 1981. Identification and mass analysis of human fibrinogen molecules and their domains by scanning transmission electron microscopy. *J. Mol. Biol.* 153:695–718.
25. Klotz, I. M. 1967. Succinylation. *Methods Enzymol.* 11:576–580.
26. Weber, K., and M. Osborne. 1969. The reliability of molecular weight determination by dodecyl sulfate-polyacrylamide gel electrophoresis. *J. Biol. Chem.* 244:4406–4411.
27. Chen, A. B., D. L. Amrani, and M. W. Mosesson. 1977. Heterogeneity of the cold insoluble globulin of plasma, a circulating cell surface protein. *Biochim. Biophys. Acta*. 493:310–322.
28. Mosesson, M. W. 1978. Structure of human plasma cold-insoluble globulin and the mechanism of its precipitation in the cold with heparin or fibrin-fibrinogen complexes. *Ann. NY Acad. Sci.* 312:11–30.
29. Hainfeld, J., J. S. Wall, and E. J. Desmond. 1982. A small computer system for micrograph analysis. *Ultramicroscopy*. 8:263–270.
30. Mosesson, M. W., and R. A. Umfleet. 1970. The cold-insoluble globulin of human plasma. *J. Biol. Chem.* 245:5728–5736.
31. Stathakis, N. E., and M. W. Mosesson. 1977. Interactions among heparin, cold-insoluble globulin, and fibrinogen in formation of the heparin-precipitable fraction of plasma. *J. Clin. Invest.* 60:855–865.
32. Stathakis, N. E., M. W. Mosesson, A. B. Chen, and D. K. Galanakis. 1978. Cryoprecipitation of fibrin-fibrinogen complexes induced by the cold-insoluble globulin of plasma. *Blood*. 51:1211–1222.
33. Wallace, D. G., J. W. Donovan, P. M. Schneider, A. M. Meunier, and J. L. Lundblad. 1981. Biological activity and conformational stability of the domains of plasma fibronectin. *Arch. Biochem. Biophys.* 212:515–524.
34. Rocco, M., R. R. Hantgen, J. Herman, and J. McDonagh. 1982. Fibronectin: cold insolubility and shape change in solution. *Circulation*. 66(Suppl. II):320*a*. (Abstr.)
35. Tooney, N. M., M. W. Mosesson, J. F. Hainfeld, and J. S. Wall. 1983. The effects of pH and surface conditions on plasma fibronectin structure. *J. Cell Biol.* 97(2, Pt. 2):323*a*. (Abstr.)

Downloaded from http://rupress.org/jcb/article-pdf/97/6/1686/1641953/1686.pdf by guest on 17 April 2024